

and codeword  $c_1 = (c_0)$  is the first transmission codeword the we obtain. If any other FEC is needed,  $c_1$  become  $c_1 = (c_0, Q)$  where  $Q$  denotes the any other FEC parity-bits. Let  $\hat{c}_1 = (\hat{c}_0)$  denotes a received first codeword. While the non-medical application receiver is finishing the communication, but the medical application receiver computes the syndrome of  $\hat{c}_0 = (\hat{D}, \hat{Q}_c)$  based on  $C_c$ .

After receiving this *NAK*, the transmitter encodes the first transmission codeword  $c_1$  with  $C_i$ , a codeword  $(c_1, Q_i)$  with  $C_i$ . Then a retransmission codeword  $c_2 = (Q_i)$ , where  $Q_i$  denotes invertible (RS) parity bits, is obtained. After that, the same operation as mentioned above is redone. Since the syndrome is nonzero, also the erroneous codeword  $\hat{c}_2$  is saved in the receiver. Once a *NAK* is sent back to the transmitter, the next retransmission word is RCPC parity bits.

The transmitter then encodes the  $c_1$  with systematic RCPC codes obtaining a codeword  $(c_1, Q_{p1})$ , where  $Q_{p1}$  denotes RCPC parity bits based on the  $c_1$ . Thus, a retransmission word  $c_{p1} = (Q_{p1})$  is generated.

After receiving  $\hat{c}_{p1}$ ,  $\hat{c}_{p1}$  is combined with  $\hat{c}_1$  obtaining a codeword  $(\hat{c}_1, \hat{Q}_{p1})$ . We can get more reliable codeword  $\hat{c}'_1$  by viterbi decoding.  $\hat{c}'_1$  is saved in the receiver and a *NAK* is sent to the transmitter even if the syndrome is nonzero. In addition, the transmitter also encodes the  $c_2$  with systematic RCPC codes obtaining a codeword  $(c_2, Q_{p2})$ , where  $Q_{p2}$  denotes RCPC parity bits based on the  $c_2$ . The same process as mentioned above is again redone. A transmitter repeats retransmission  $c_1, c_2, c_{p1}, c_{p2}$  until the message  $D$  is error-free and consequently accepted.

We can see later from the results that when a receiver has a function of decoding with a reliability of decoded codeword based on  $C_i$ , the system throughput can achieve more improvement. It is our future work.

#### 4. Performance Evaluation

Figures 7-12 show the performances of our proposed system using RCPC-based, RS-based and concatenated-based H-ARQ. Simulation parameters for RCPC-based H-ARQ and invertible codes-based H-ARQ are given in Table 2.  $I$  and  $I_{max}$  denote the number of transmission and the max number of transmission, respectively.

We assume the throughput efficiency is computed by

$$\eta = (1 - PER) * (K/N), \quad (3)$$

where  $PER$  denotes packet error rate,  $K$  and  $N$  denote transmitted message bits length and total transmitted message bits length, respectively. Hence, the throughput efficiency shows the average of error-free data communications.

And we define the data rate as the number of data

bits per second. With coding, the parity bits are also transmitted, so the data rate is not equal to the bit rate. For the non-medical communication, the data rate is the same as the bit rate, because the first transmitting codeword contains only the parity bits of CRC codes.

For comparing, the results of convolutional codes with code rate of 1/3 and the constraint length of 3 are shown.

**Table 2** Simulation parameters for RCPC-based, RS-based and proposed concatenated based H-ARQ.

Channel	IEEE802.15.6 CM3 and CM4
Mod. Demod.	2PPM, Energy detection
Pulse shape	modulated RRC
Pulse duration	2 nsec
Bit rate	2 Mbps
CRC	CRC-CCITT (parity length 16 bits)
FEC (RCPC based)	constraint length : 3 parent code rate : 1/3 code rates : $R_k=1, 2/3, 1/3$
Decoding	Hard Decision Viterbi decoding
FEC (RS codes)	GF(2 <sup>4</sup> ), (15,7)RS codes GF(2 <sup>5</sup> ), (31,15)RS codes
Decoding	Bounded distance decoding
FEC (concatenated-based)	RCPC codes: constraint length : 3 parent code rate : 1/2 code rates : $R_k=1, 1/2$
Decoding	RS codes: the same as RS-based the same as RCPC-based and RS-based
Block length	330 bits (contain CRC parity)
Max. No of retransmissions	RCPC-based : 1, 2 RS-based : 1 concatenated-based : 1,2,3

**Table 3** HRO-RCPC codes of parent code rate 1/3

$(g_0, g_1, g_3)$	$P_1$	$P_{2/3}$	$P_{1/2}$	$P_{2/5}$	$P_{1/3}$
(5,7,7)	0 0	0 1	1 1	1 1	1 1
	1 1	1 1	1 1	1 1	1 1
	0 0	0 0	0 0	0 1	1 1

##### 4.1 Performance Evaluation

Figures 7 and 8 show the good performance of the RCPC-based H-ARQ ( $I=3$ ) as its achieved the bit error rate  $BER=10^{-6}$  at  $SNR=11.6$  dB due to its viterbi decoding and code rate. Under  $SNR=14$  dB, because of the fail decoding, the  $BER$  of the first transmission of the RCPC-based one is higher than the non coded one. The non coded one is the first transmission of the RS-based, the concatenated-based one The BER of non coded one is equal to  $10^{-3}$  at  $SNR=13$  dB. Also the RS-based ( $I=2$ ), the RCPC-based ( $I=2, 3$ ) and the concatenated-based ( $I=2, 3, 4$ ) achieved  $BER=10^{-6}$  at  $SNR=13$  dB. Therefore, the medical communications can satisfy its QoS by using H-ARQ function while the bit rate is note changed.

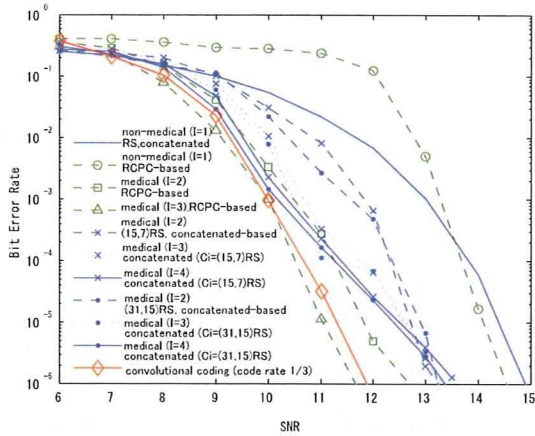


Fig. 7 Bit error rate for medical and non-medical applications in the CM3 channel.

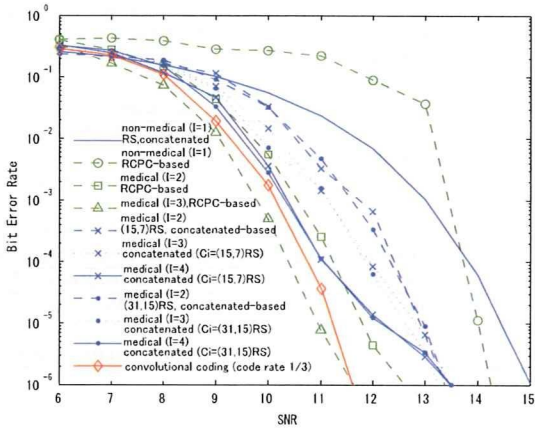


Fig. 8 Bit error rate for medical and non-medical applications in the CM4 channel.

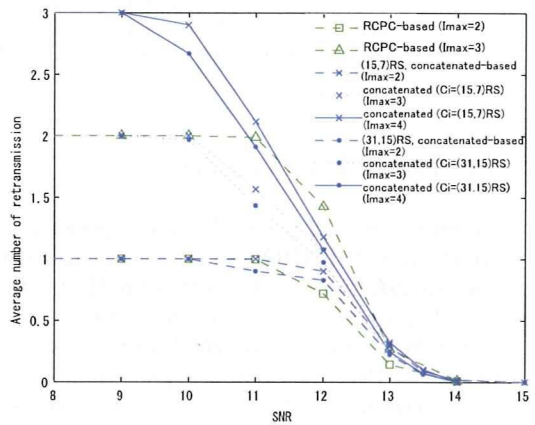


Fig. 9 Average number of retransmission for medical applications in the CM3 channel.

From figures 9-12, at the low  $SNR$ , because of the  $PER$  of the RCPC-based ( $I=3$ ) is very low, the throughput efficiency of the RCPC-based ( $I=3$ ) is bet-

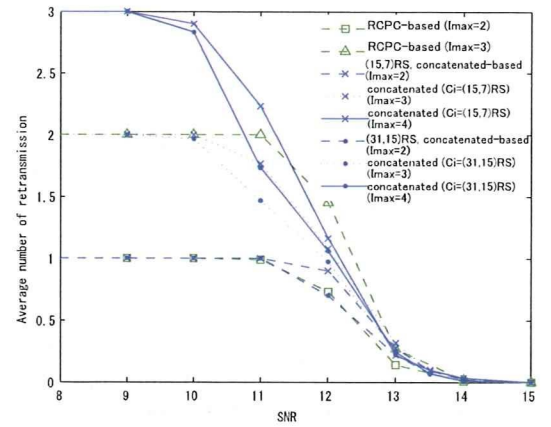


Fig. 10 Average number of retransmission for medical applications in the CM4 channel.

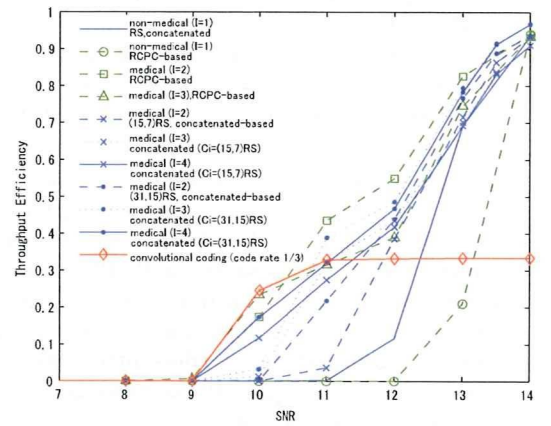


Fig. 11 Throughput vs SNR for medical and non-medical applications in the CM3 channel.

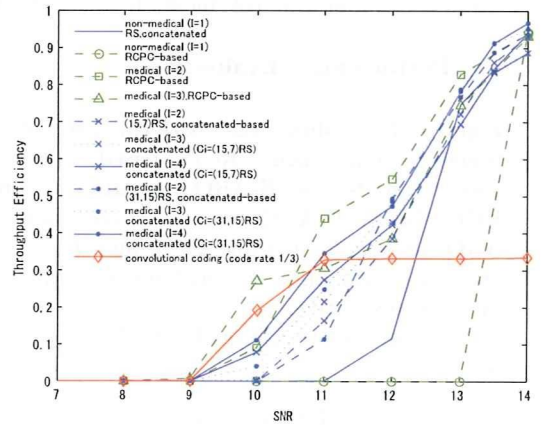


Fig. 12 Throughput vs SNR for medical and non-medical applications in the CM4 channel.

ter than the RS-based ( $I=2$ ) and the concatenated-based ( $I=2, 3, 4$ ). But over  $SNR=14$  dB, the average number of retransmission of the RCPC-based ( $I=3$ )

is larger than the RCPC-based ( $I=2$ ), the RS-based ( $I=2$ ) and the concatenated-based ( $I=2, 3, 4$ ), so the throughput efficiency of the RCPC-based ( $I=3$ ) is low.

At the first retransmission, the information and CRC parity bits length of every codewords are the same. Then, at the high  $SNR$ , all cases achieve the same throughput efficiency. And the average number of retransmission also converges. Hence, the proposed scheme adapts to the channel.

The performance when only using convolutional codes with code rate  $1/3$  also achieves the good  $BER$  performance. But if the bit rate remains  $2Mbps$ , the data rate becomes  $2/3Mbps$ . Furthermore, the throughput efficiency is still  $1/3$  at the high  $SNR$ .

To summarize, the RCPC-based H-ARQ has the best performance. However, the non-medical receiver needs to have the function of viterbi decoding, because the RCPC codes of the RCPC-based used in this study is not the systematic codes. Moreover, the  $BER$  of the first transmission of the RCPC-based is very high at the low  $SNR$ . So the proposed concatenated scheme is more suitable for the low complexity of the non-medical receivers and the high reliability of the medical communications.

## 5. Conclusions

This research work explored hybrid type II ARQ techniques for BANs. The signaling scheme was IR-UWB in the high band of UWB with 2PPM and energy detection. The investigated H-ARQs were based on generic HRC-RCPC and invertible RS codes combined with simple CRC. We employed concatenated codes based H-ARQ to achieve both of high data rate of the non-medical application and low bit error rate of the medical one.

Simulation results show that good performance in UWB-BAN channels can be achieved. Hence, a robust scheme is possible for the medical applications of BANs. The advantage of this scheme is less complex and consequently less power consumption plus it achieves higher throughput than when only the FEC was used, which are important for BAN applications. Finally, the proposed schemes showed a practical form of coexistence between the medical and the non-medical applications in BANs.

## References

- [1] *Body Area Network Channel Model Document*, IEEE P802.15-08-0780-0x-0006, [Online] Available: <https://mentor.ieee.org/802.15/documents>.
- [2] J. Hagenauer, "Rate-Compatible Punctured Convolutional Codes", *IEEE Transactions on Communications*, Vol 36, No 4, April 1988, pp. 389-400.
- [3] P. Frenger, et.al, "Multi-Rate Convolutional Codes", *Technical Report 21*, Department of Signals and Systems, Chalmers University, Sweden, April 1998.
- [4] S. Falahati, et.al., "Convolutional Coding and Decoding in Hybrid Type II ARQ Schemes on Wireless Channels", *IEEE Vehicular Technology Conference*, 1999, pp. 2219-2224.
- [5] R. Prasad, M. Ruggieri, *Technology Trends in Wireless Communications*, Artech House Publishers, April 2003, ISBN-10: 1580533523.
- [6] S. Lin, P. Yu., "A Hybrid ARQ with Parity Retransmission for Error Control of Satellite Channels", *IEEE Transactions on Communications*, Vol 30, No 7, July 1982, pp. 1701-1719.
- [7] S. Lin, D. J. Costello Jr., *Error Control Coding: Fundamentals and Applications*, Prentice-Hall, Englewood Cliffs NJ, 1983.

**Haruka Suzuki** was born in Akita, Japan, in 1986. She received the Bachelor's degree in Electrical and Computer Engineering from Yokohama National University, Yokohama, Japan, in 2009. She is currently working toward the M.S. degree in Electrical and Computer Engineering at Yokohama National University, Yokohama, Japan. Her research interests include ultra-wideband communications, channel coding in wireless communications and information theory. She is a student member of the IEICE.

**Marco Hernandez** received a M.S. in Electrical Engineering in the Center for Research and Advanced Studies of the National Polytechnic Institute of Mexico (CINVESTAV), and a Ph.D. degree in Electrical Engineering from Delft University of Technology in The Netherlands. From 1995 to 1996, he was an International Young Graduate Trainee with the European Space Research and Technology Center (ESTEC) in The Netherlands working on land mobile satellite propagation channel modeling. From 1997 to 2001 he was a research assistant with the Faculty of Electrical Engineering, TVS Group, Delft University of Technology. In 1999 he had a research internship in the Center for Communications and Signal Processing Research Laboratory (CCSPR) at New Jersey Institute of Technology, USA. From 2001 to 2002 he was a research assistant with the Mobile Communication Group at Institute Eurecom in Sophia-Antipolis, France. From 2003 to 2006 he was a research associate in the Center of Excellence (COI) (Graduate School of Electrical Engineering) of Yokohama University, Japan. In 2007, he joined the National Institute of Information and Communications Technology (NICT) as senior researcher in the Medical Information and Communications Technology Group. His research interest is in wireless communications.

**Ryuji Kohno** received the Ph.D. degree from the University of Tokyo in 1984. Dr. Kohno is currently a Professor of the Division of Physics, Electrical, and Computer Engineering, Yokohama National University. In his career, he was a director of Advanced Telecommunications Laboratory of SONY CSL during 1998-2002 and currently a director of UWB Technology institute of National Institute of Information and Communications Technology (NICT). In his academic activities, he was elected as a member of the Board of Governors of IEEE Information Theory (IT) Society in 2000 and 2003. He has played

a role of an editor of the IEEE Transactions in IT, Communications, and Intelligent Transport Systems (ITS). He is fellow of IEICE, vice-president of Engineering Sciences Society and IEICE and has been the Chairman of the IEICE Technical Committee on Spread Spectrum Technology, that on ITS, and that on Software Defined Radio(SDR). Prof. Kohno has contributed for organizing many international conferences, such as an chair-in honor of 2002 & 2003 International Conference of SDR (SDR'02 & SDR'03), a TPC co-chair of 2003 IEEE International Symposium on IT(ISIT'03), that of joint UWBST & IWUWB'04 and IWUWB'05, and so on. He was awarded IEICE Greatest Contribution Award and NTT DoCoMo Mobile Science Award in 1999 and 2002, respectively.

# Frequency Dependent Dispersion Compensation Method of Electromagnetic Waves Hyperthermia Using Time Reversal Waves

Hideaki Miura, Ryuji Kohno

*Division of Physics, Electrical and Computer Engineering, Yokohama National University  
79-5 Tokiwadai, Hodogaya, Yokohama, 240-8501, Japan  
Tel: +81-45-339-4116, Fax: +81-45-338-1176  
E-mail: hideaki@kohnolab.dnj.ynu.ac.jp, kohno@ynu.ac.jp*

## Abstract

*Recently, the increase of female death rate of breast cancer is significant. The treatments for cancer are surgery, medication, radiation and chemical therapy, whereas these treatments are very aggressive interventions. Therefore, attentions are currently focused on hyperthermia as a less invasive approach. Hyperthermia is a treatment which uses the characteristic that cancer tissue becomes necrotic at a lower temperature than normal tissue. In this paper, we use the hyperthermia treatment using electromagnetic time reversal (TR) waves. The invariance of the wave equation under time reversal enables optimal refocusing by TR arrays. However, in lossy or dispersive media, such as human body, time invariance is lost and TR techniques can be degraded. To alleviate this problem, we propose frequency dispersion compensation method which use short time Fourier transform (STFT) and the S-parameter. Additionally, we present examples of temperature distributions calculated using bio-heat equations. The proposal method is shown to improve refocusing and to achieve sufficiently elevated temperatures in the vicinity of small cancer while maintaining safe temperatures throughout the remainder of the normal breast.*

## 1. Introduction

Recently, cancer account for about 30 percent of total deaths in Japan. The number of patients with cancer is increasing yearly. Breast cancer is one of the most general types of cancer among women. The common treatment for cancer typically involves a lumpectomy or partial mastectomy to remove the cancer tissues and its margins normal tissues. It follows medication, radiation and chemical therapy whereas these treatments are very aggressive interventions. In particular, post-treatment Quality of Life (QoL) is emphasized in breast cancer of women. Therefore, attentions are currently focused on hyperthermia as a less invasive approach [1].

Hyperthermia is treatment which uses the characteristic that cancer tissue becomes necrotic at a lower temperature than normal tissue. This treatment raises the temperature in the cancer volume above 42.5°C in order to provoke cancer tissue's death and is necessary to use a method for focusing on

affected areas effectively avoiding heating other areas. In order to solve above problems, our system uses time reversal waves. Additionally, we propose frequency dispersion compensation method since human body is a frequency dispersion lossy medium. The breast region has different characteristic from other regions, the dielectric constant is higher in cancer than in surrounding breast fat. Thus, strong scattered waves are caused around cancer region. For this reason, TR waves can be applied for hyperthermia.

One element of antennas transmits a pilot signal which is UWB mono pulse, and all elements antenna receive scattered waves. Next, received waves applied to time reversal operation are retransmitted from all elements antenna. Consequently, retransmitted waves refocus automatically on the region where scattered waves generated [2]. However, TR waves cannot be applied directly since the breast is a frequency dispersion loss medium. Therefore, we propose method for compensating dispersive effect in order to improve the refocusing of TR waves. Compensated TR waves are tightly refocused on cancer areas and less invasive to normal tissue areas.

This paper is organized as follows: In Section 2, the principle of hyperthermia using TR waves is described. Some basic characteristic of electromagnetic wave propagation and proposal method of frequency dispersion compensation are presented in Section 3. In Section 4, we discuss the calculation of SAR and temperature increment. In Section 5, we evaluate the proposed method. Finally, conclusions are given and we describe future works in Section 6.

## 2. Hyperthermia Treatment Using Time Reversal Waves

Hyperthermia is a kind of cancer treatment in which body is exposed locally to high temperatures by irradiating electromagnetic waves, magnetic fields or ultrasound waves. Figure.1 shows survival rate in cancer tissue exposed 41[°C] to 44[°C]. It shows that above 42.5[°C], survival rate in cancer tissue is obviously decreased in an exponential manner.

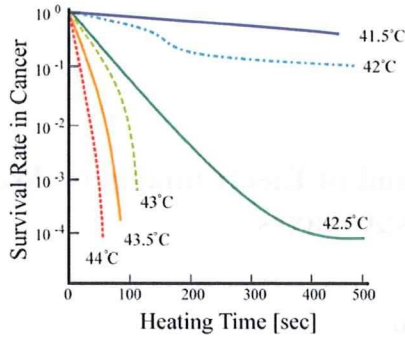


Figure 1- Survival rate of cancer tissue

In this paper, we use electromagnetic TR waves as a method of making a focus point. The TR focusing approach is closely related to the matched-filter principle used in signal processing. This principle is that the output of a given linear system whose impulse response is  $h(t)$  is maximized with an input signal with form  $h(-t)$ . The response results from the convolution  $h(t) \otimes h(-t)$ . It is an even function whose maximum is reached at  $t=0$  and is given by the energy of the input signal.

We show procedures of TR operation in mathematical expressions. Firstly, pilot signal  $p(t)$  of mono pulse is transmitted. Pilot signal is propagated in the medium between the breast and cancer tissues from  $i$ th element of pilot signal transmit antennas. Secondly, the signal is scattered around cancer region and  $j$ th antenna receives backscattered waves. Therefore, the received wave at  $j$ th element of antennas  $R_j$  is given by

$$\begin{aligned} R_j(\mathbf{r}_j, t) &= f(t) \otimes h_j(\mathbf{r}_j - \mathbf{r}_0, t) \\ f(t) &= p(t) \otimes h_0(\mathbf{r}_0 - \mathbf{r}_i, t) \otimes \xi(t) \end{aligned} \quad (1)$$

where  $\xi$  is a reflection coefficient at cancer region. Our TR-algorithm applies to point scatter approximation in reflections at cancer region. Therefore backscattered wave is radiated from cancer region treating as a point source. These received waves include reflections from skin and direct waves from pilot signal transmitting antenna. We use hanning window in order to extract direct waves from the cancer region. The window length is determined approximately from the duration of the pilot signal. The offset times of this window are estimated by calculating a propagation delay time between the cancer location and elements. The cancer location is assumed to be estimated accurately by priori information. Propagation delay time is calculated by propagation distance and propagation velocity [3]. Propagation velocity is given by

$$v = \frac{C}{\epsilon_{ave}} \quad (2)$$

Here,  $C$  is a velocity of light and  $\epsilon_{ave}$  is relative permittivity of the average normal breast tissue. TR operated retransmitting waves are expressed by

$$T_j^{TR}(\mathbf{r}_j, T-t) = f(T-t) \otimes h_j(\mathbf{r}_j - \mathbf{r}_0, T-t). \quad (3)$$

This time-reversed wave transmitted by  $j$ th antenna. TR operated retransmitting wave is propagated in the breast medium and this propagated waves at position  $\mathbf{r}$  is expressed by

$$R_0^{TR}(\mathbf{r}, T-t) = f(T-t) \otimes h_j(\mathbf{r}_j - \mathbf{r}_0, T-t) \otimes h_j(\mathbf{r} - \mathbf{r}_j, t). \quad (4)$$

This equation is related to the matched-filter principle. If the position and time are  $\mathbf{r}=\mathbf{r}_0$  and  $t=T$ , the electric field is maximum value. Breast tissue has frequency dependent attenuation and dispersion. Time-reversal in lossy and dispersive background medium, time-reversal invariance is broken. Therefore compensation techniques become necessary for time-reversal.

### 3. Compensation Method of Frequency Dispersion and Attenuation

As mentioned previous section, TR operation in frequency dependent dispersive medium such as human body cannot be compensated attenuation. In this section, we proposed the compensation method based on STFT and the S-parameter.

#### 3.1. Electromagnetic Characteristic of Breast Tissues

A human body consists of various organs with complex structures. Furthermore, each organ has different characteristics of frequency dependent conductivity and permittivity. Indeed, the electromagnetic wave propagation in dispersive biological tissues is frequency dependent conductivity and permittivity. The dispersion characteristics are modeled using single pole Debye dispersion equations of the following form:

$$\epsilon_r(\omega) = \epsilon_\infty + \frac{\epsilon_s - \epsilon_\infty}{1 + j\omega\tau} - j \frac{\sigma_s}{\omega\epsilon_0}. \quad (5)$$

Here,  $\epsilon_\infty$  is the relative permittivity at infinite frequency,  $\epsilon_s$  is the static relative permittivity,  $\sigma_s$  is the static conductivity, and  $\tau$  is the relaxation time constant. These parameters are different for body tissues. Then, the relative permittivity is the real part of complex permittivity, and the imaginary part is the conductivity. Generally, the higher percentage of water content the tissue have, the higher the value of relative permittivity and conductivity is, then electromagnetic waves attenuation will be significant.

The S-parameter is an analytical model of the frequency response associated with propagation distance [4]. We assume that each antenna is an infinite line source of electric current located at  $\mathbf{r}_n$  in a uniform medium of normal breast tissue. We treat the scatter as a conducting circular cylinder of infinite

length and infinitesimal radius compared to the small breast legion, the transfer function is given by

$$S_n(\mathbf{r}, \omega) = \frac{1}{\sqrt{|\mathbf{r} - \mathbf{r}_n|}} e^{-(\alpha(\omega) + j\beta(\omega))|\mathbf{r} - \mathbf{r}_n|} \quad (6)$$

where  $\mathbf{r}_n$  is position vector of antenna and  $\alpha$  is the frequency-dependent attenuation factor and  $\beta$  is the frequency-dependent phase constant [5]. These two factors are calculated by the following equations.

$$\alpha(\omega) = \omega \sqrt{\mu \epsilon} \sqrt{\frac{1}{2} \left( \sqrt{1 + \left( \frac{\sigma}{\omega \epsilon} \right)^2} - 1 \right)} \quad (7)$$

$$\beta(\omega) = \omega \sqrt{\mu \epsilon} \sqrt{\frac{1}{2} \left( \sqrt{1 + \left( \frac{\sigma}{\omega \epsilon} \right)^2} + 1 \right)} \quad (8)$$

The attenuation of transfer function depends on the distance and frequency. The transfer function  $S_n(\mathbf{r}, \omega)$  is obtained from the distance between the cancer and the  $i$ th antenna which is known by priori information.

### 3.2. Proposed Compensation Method of Frequency Dispersion Attenuation

In general terms, a dispersive medium acts as a filter for propagating signals. To compensate dispersive effect, an inverse filter should be constructed. In order to obtain this filter, transfer function in dispersive medium is needed. But, it is difficult to know the transfer function preliminarily since the human body is formed of various organs with complex structures. Therefore, we estimate the transfer function in human body using S-parameter with electric constants of an average human body and priori information of cancer position. Since dispersion effects are cumulative, the filters associated with signal components corresponding to different effective propagation distance. Therefore, received signals which propagated long distance in breast model need stronger compensation than those propagated short distance. Ideally, different filters should be applied for each particular instant, but it is impractical. It is more convenient to time-window the received signals and apply different filters to each windowed signal. We apply a short-time Fourier transform (STFT) to receive signals. The discrete STFT is described following equation.

$$X[k, i] = \sum_n x_i[n] \omega_i[n] e^{-j \frac{2\pi}{L} nk}, i = 1, \dots, M \quad (9)$$

where  $\omega_i$  is the  $i$ th hamming window, width of this window is 256 steps, overlapping factor is 0.5.  $L$  is the Fourier transform length, and  $M$  is the total number of windows. In frequency domain, the filtering carried out by

$$Y[k, i] = \frac{X[k, i] T(\omega_k)}{S(\mathbf{r}, \omega_k)} \quad (10)$$

where  $S(\mathbf{r}, \omega_k)$  is the  $i$ th transfer function,  $T(\omega_k)$  is the pilot signal in the frequency domain. In order to excessively amplify the high frequency band, we apply to pilot signal as a stabilization operator. Finally, dispersion-compensated signal is obtained by an inverse STFT. The inverse STFT is described as follows

$$x_c[n] = \sum_{i=1}^M \frac{1}{\omega_i[n]} \sum_k Y[k, i] e^{j \frac{2\pi}{L} nk} \quad (11)$$

A block diagram of the proposed process is given in Figure 2.

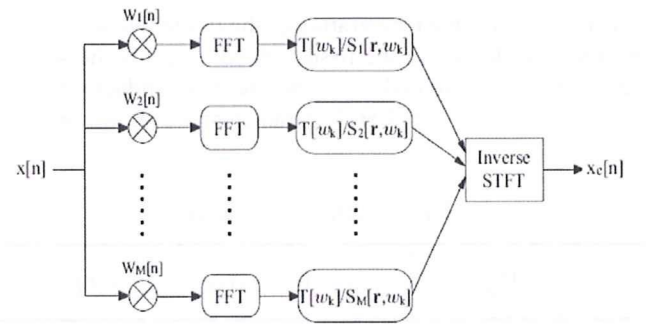


Figure 2-Block diagram of compensation method

## 4. Simulation Model for Performance Evaluation

In this section, we show the simulation model of hyperthermia system using 2-D simulations to calculate distributions of absorbed SAR and temperature throughout the breast. At first, the 2-D simulation system is shown in Figure 3. This model is assumes sliced breast model and 16 antennas located on circular.

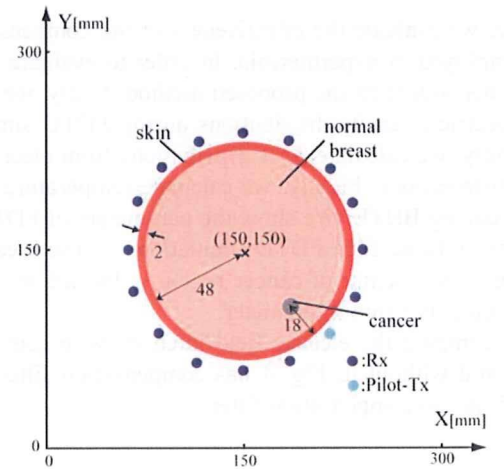


Figure 3-Numerical breast model

We calculate integration of electric intensity, SAR and temperatures during FDTD simulations. The specific absorption

rate (SAR) is the rate at which electromagnetic energy is absorbed by tissues per unit weight. The relationship between electric field and SAR is given by

$$SAR = \frac{\sigma}{\rho} |E|^2 [W/kg] \quad (12)$$

where  $\sigma$  is the electric conductivity of the tissue,  $E$  is the electric field, and  $\rho$  is the density of tissue.

The thermal model of human body is based on Pennes bio-heat equation (BHTE) [6]. This is used to simulate the temperature profile from SAR. The equation is expressed as

$$\rho c \frac{dT}{dt} = \kappa \nabla^2 T - \rho \rho_b c_b F(T - T_b) + \rho SAR \quad (13)$$

where  $T(T_b)$  is the temperature of the tissue (blood),  $\rho(\rho_b)$  is the physical density of the tissue (blood),  $c(c_b)$  is the specific heat of the tissue (blood),  $\kappa$  is the thermal conductivity,  $F$  is flow rate of blood. The BHTE parameters are shown in Table 1.

Table 1-BHTE parameter

	$\rho$ [kg/m <sup>3</sup> ]	$c$ [J/kg/°C]	$\kappa$ [W/m/°C]	$F$ [m <sup>3</sup> /kg/s]
Breast fat	$0.94 \times 10^3$	$2.3 \times 10^3$	0.20	$0.14 \times 10^{-6}$
Cancer	$1.07 \times 10^3$	$3.5 \times 10^3$	0.59	$0.13 \times 10^{-6}$
Skin	$1.0 \times 10^3$	$3.5 \times 10^3$	0.44	$1.3 \times 10^{-6}$
Blood	$1.06 \times 10^3$	$3.9 \times 10^3$	14.0	

## 5. Computer simulation result

Here, we evaluate the effectiveness of the compensation filter employed in hyperthermia. In order to evaluate the focus point dependent on the proposed method, firstly, we calculate the electric intensity distributions during FDTD simulations. Secondly, we calculate SAR distributions from electric intensity distributions. Finally, we calculate temperature distributions during BHTE. We show the parameters of FDTD simulations in Table 2. In FDTD simulation, we use breast model of Fig. 3 and center of cancer region is located at (170,175) and cancer is 5 mm in diameter.

We compare the electric field intensity with compensation filter and without it. Fig. 4 has compensation filter applied. Fig. 5 has no compensation filter.

Table 2-Parameters in FDTD Simulation

Dispersive Model	Debye Model
Analytic Space	300×300[cell]
Cell Size	1.0×1.0[mm]
Time Step	2.1228[psec]
Pilot Signal	Derivative Gaussian Mono Pulse (Bandwidth=1-11[GHz])

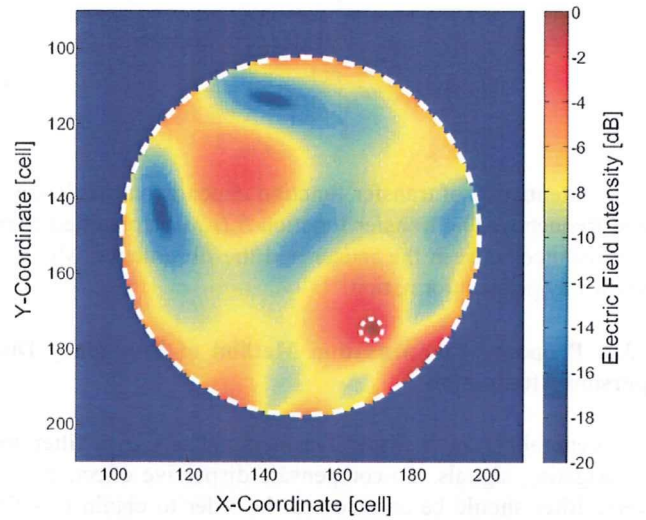


Figure 4-Electric Intensity Distribution (Compensated)

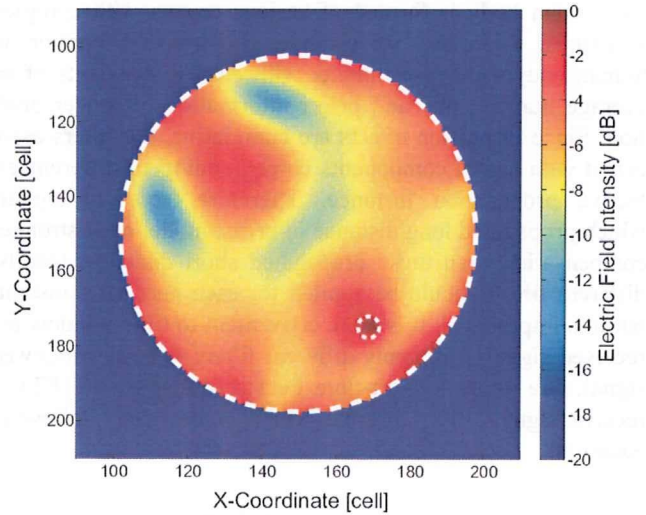


Figure 5-Electric Intensity Distribution (Not Compensated)

Fig. 4 represents that in the case of applied compensation filter, the focal point is more sharp compared to the case of not applied filter. Additionally, applied compensation method of electric intensities in normal breast region is lower than



not applied in normal breast region. Therefore, in order to be less invasive, proposed compensation method is effective.

We calculate temperature distributions and show the parameters of BHTE simulation in Table 3.

Table 3-Parameters in BHTE Simulation

Time Step	0.5[sec]
Analytic Space	300×300[cell]
Analytic Time	1800[sec]
Cell Size	1.0×1.0[mm]
Initial Temperature of Model	30.0[°C]

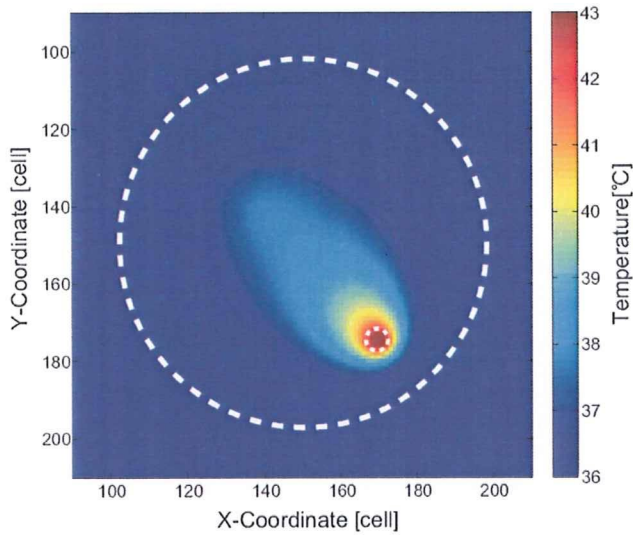


Figure 6-Temperature Distribution applied Compensation method

Fig. 6 shows that the result of temperature distribution applied compensation method. It shows that, temperatures in cancer region are above 42.5[°C] and in normal breast tissue region, temperatures are below 42.5[°C]. This characteristic of temperature is found to be useful for hyperthermia treatment.

## 6. Conclusions

In this paper, we analyze the electric intensity and temperature distribution in numerical breast model and we propose dispersive attenuation compensation method since TR operation in dispersive medium such as human body is degraded and time invariance is lost. Firstly, we analyze the distribution of electric intensity. As a result, TR operation applied compensation method is sharper in focal pointing the cancer region. Additionally, we analyze temperature distribution using TR operation applied compensation method. This temperature distribution shows that temperatures in cancer region

and normal breast region are suitable for hyperthermia treatment.

## 7. References

- [1] M. C. Converse, E. J. Bond, S. C. Hagness, and B. D. Van Veen, "Ultrawideband microwave space-time beamforming for hyperthermia treatment of breast cancer: A computational feasibility study," *IEEE Transactions on Microwave Theory and Techniques*, vol. 52, no. 8, pp. 1876-1889, August 2004.
- [2] G. Lerosey, J. de Rosny, A. Tourin, A. Derode, G. Montaldo, and M. Fink, "Time reversal of electromagnetic waves." *Physical Review Letters*. vol. 92, no. 19, pp. 233-235, May, 2004.
- [3] Mehmet E. Yavuz, Fernando L. Teixeira, "Frequency Dispersion Compensation in Time Reversal techniques for UWB Electromagnetic Waves", *IEEE Geoscience and Remote Sensing Letters*, vol.2, no.2, pp.233-237, April 2005.
- [4] M. Lazebnik, M. Okoniewski, J. H. Booske, and S. C. Hagness, "Highly accurate Debye models for normal and malignant breast tissue dielectric properties at microwave frequencies," *IEEE Microwave and Wireless Components Letters*, vol. 17, no. 12, pp. 822-824, Dec. 2007.
- [5] T. Ohmori, "Bio electromagnetic engineering and application," Fujitec Corporation.

# Study on Medical and non-Medical UWB Transmission Schemes in Wearable Body Area Network

Hideki MOCHIZUKI<sup>†\*</sup>, *Student Member* and Ryuji KOHNO<sup>†\*\*</sup>, *Fellow*

**SUMMARY** In this paper, we proposed a new system for wearable WBAN and compare conventional coherent low data rate IR UWB (DS-UWB, Chirp on UWB) and our proposed system of pulsed chirp UWB with frequency hopping (single hop or parallel hop). We proposed single hop Pulsed UWB system for high reliable system. And, to consist medical system with non-medical system, we proposed parallel hop Pulsed chirp UWB system. IEEE 802.15.6BAN channel model has been utilized for BER evaluation under multi pico-net interference conditions. Our results show that proposed pulsed chirp UWB with frequency hopping has superior performance compared to conventional methods.

**key words:** *Body Area Network, Ultra Wide Band, Frequency Hopping*

## 1. Introduction

Recently, there has been considerable amount of research effort directed towards applied information and communications technology to medical services [1]. As main concept, WBAN (Wireless Body Area Network) has been researched. WBAN are networks composed of wireless communication inside, outside or between inside and outside of a human body. Communication between devices located outside of a human body is called wearable WBAN; similarly, Communication between devices located inside of a human body is called implanted BAN. In this paper, we will limit our discussion to wearable WBAN.

Wearable WBAN is expected to have numerous applications for medical use and non-medical use. And wearable WBAN is consistent of small, autonomous network devices, the consequent low transmission power is required for their longer battery life.

Vital signs are important information, so it is important to achieve privacy. Furthermore, considering practical purposes and non-medical use, it is necessary to achieve higher data rates. On the other hand, a lot of attention has been paid to UWB (ultra wideband) wireless communications systems due to their great potential to reach high data rates and to simplify the RF circuitry of the transceivers and lower the transmit power in wireless communications. These features correspond with the demand for the wearable WBAN communications. Since we proposed new UWB system.

We proposed new UWB schemes which have been able to be high speed communication and have patiento to multi pico-net interference by using frequency hopping.

In this paper, we compare conventional low data rate IR UWB (DS-UWB, Chirp on UWB) and our proposed system of pulsed chirp UWB with frequency hopping (single of parallel hop). IEEE 802.15.6BAN channel model has been utilized for BER evaluation under multi pico-net interference conditions.

This psper is organaized as follows: In Sect.2, conventional UWB communication technology which is DS-UWB and Chirp on UWB. In Sect.3, proposed method which is used single hop is described. Proposed method which is used parallel hop is described in Sect.4. Characteristics of wearable WBAN are described in Sect.5. Simulation results are drawn in Sect.6. Finally, conclusions are delineated in Sect.7.

## 2. UWB communication technology

### 2.1 DS-UWB system

#### 2.1.1 Transmitter's Description

The transmitted signal for DS-UWB using the spreading sequence of the sequence length  $N_s$ , denoted  $f(t)$ , is given by

$$f(t) = \sum_{j=0}^{N_s} m_j \delta(t - jT_f) \quad (1)$$

Here,  $\delta(t)$  represents the transmitted monocycle waveform,  $m_j$  is the  $j$ -th component of the spreading sequence and  $T_f$  is the time frame. We assume that  $f(t)$  consists of  $N$  pulses.

#### 2.1.2 Receiver's Description

The received signal  $f_{rec}(t)$  is represented by

$$f_{rec}(t) = \sum_{j=0}^{N_s} m_j \delta(t - jT_f) + n(t) \quad (2)$$

Where  $n(t)$  represents additive white Gaussian noise (AWGN) and multiuser interference (MUI). At the receiver, the spreading sequence is assumed to be known and the template function to be correlated with the

received signal is assumed to be the same as the transmitted signal. Thus the replica signal generated at the receiver,  $f_{rep}(t)$  is given by

$$f_{rep}(t) = \sum_{j=0}^{N_s-1} m_j(\delta(t - iT_f)) \quad (3)$$

The correlation function  $R(\tau)$  between  $f_{rec}(t)$  and  $f_{rep}(t)$  is calculated as

$$R(\tau) = \int f_{rec}(t)f_{rep}(t + \tau)dt \quad (4)$$

Transmitted symbol is decided by calculating  $R(\tau)$ .

## 2.2 Chirp on UWB system

The chirp waveform is represented by

$$s(t) = \begin{cases} \cos(\theta(t))(0 \leq t \leq T) \\ 0(\text{otherwise}) \end{cases} \quad (5)$$

$\theta(t)$  is the change of phase depending on time and  $T$  is time duration. In the case of liner chirp, chirping rate  $\mu(t)$  is constant so that frequency  $f_M(t)$  is liner function with the respect to  $t$  and  $\theta(t)$  is a quadratic function.

$$f_M(t) = f_0 + \mu(t) \quad (6)$$

$$s(t) = \cos(2\pi f_0 t + \pi \mu t^2) \quad (7)$$

Band width  $B$  is a function of time duration  $T$  and chirping rate  $\mu$ .

$$B = |\mu|T \quad (8)$$

Chirp on UWB waveform is made by multiplying root raised cosine pulse and linear chirp. Root raised cosine pulse  $r(t)$  is represented by

$$r(t) = \frac{4\beta}{\pi\sqrt{T_p}} \frac{\cos\left[\frac{(1+\beta)\pi t}{T_p}\right] + \frac{\sin\left[\frac{(1-\beta)\pi t}{T_p}\right]}{\frac{4\beta t}{T_p}}}{\left(\frac{4\beta t}{T_p}\right)^2 - 1} \quad (9)$$

$\beta = 0.6$  is roll-off factor. Using this pulse, Chirp on UWB waveform is represented by

$$P_{CoU}(t) = \begin{cases} r(t)\exp(-j\frac{\pi\mu t^2}{2})(-\frac{T}{2} \leq t \leq \frac{T}{2}) \\ 0(\text{otherwise}) \end{cases} \quad (10)$$

### 2.2.1 Chirp on UWB system model

In this section, we describe Chirp on UWB system.

Data  $b(t)$  was modulated by chirp waveform  $P_{CoU}(t)$ . Transmitted waveform  $s(t)$  is represented by

$$s(t) = b(t)c(t) \quad (11)$$

Each user is assigned a frequency band of 500 MHz and positive or negative chirp slope, as defined in table. 1. Description of the Chirp on UWB receiver is the same as DS-UWB one.

**Table 1** User assigned bands and chirping slopes.

user	chirping rate	$f_c$ [GHz]
1	$\mu > 0$	3.25
2	$\mu < 0$	3.25
3	$\mu > 0$	3.75
4	$\mu < 0$	3.75
5	$\mu > 0$	4.25
6	$\mu < 0$	4.25
7	$\mu > 0$	4.75
8	$\mu < 0$	4.75

## 3. Pulsed Chirp UWB method (Parallel hop)

Pulsed Chirp UWB method's aim is to be able to be higher reliable communication for medical and high speed communication for non-medical than conventional system by using hopping sequence. Since, in this section, we describe proposed Pulsed Chirp UWB methods which consist medical system and non-medical system by using parallel hop.

In this system, if one user uses one subband, we call this proposed method single hop. On the other hand, one user uses multi subband, we call proposed method parallel hop. If we use parallel hop for medical system, each subbands are assigned same data and demodulate by majority rule to be able to be high reliable communication. If we use parallel hop for non-medical system, each subbands are assigned different data, so it's able to be high data rate communication. Thus, this proposed method is able to consist medical with non-medical system. Thereinafter, we describe this system's details.

Transmitted waveform  $f(t)$  is

$$f(t) = \sum_{k=1}^{d_s} \sum_{j=0}^{N_s-1} m_{i,j}d(k)(s_{i,k,j}(t - jT_f)) \quad (12)$$

$$(c_{i,j} = 1 \rightarrow m_{i,j} = 1, c_{i,j} = 0 \rightarrow m_{i,j} = -1)$$

$T_f$  is time frame,  $c_{i,j}$  is j-th element of PN sequence assigned to the i-th user;  $N_s$  is the length of the PN sequence,  $d_s$  is the count of parallel transmitted data. If we use single hop method, we defined  $k = 1$ . Similarly,  $s_{i,k,j}$  is a waveform of the j-th corresponding pulse for the i-th user which is k-th parallel transmit signal.

Chirp pulse waveforms  $s_{i_k,j}$  are described in detail below. First, maximum and minimum value of used frequency is defined -  $f_{max}$  and  $f_{min}$  respectively. Second, we divide the bandwidth by applied length of sequence. Bandwidth  $B$  and chirped bandwidth  $\Delta f$  are

$$B = f_{max} - f_{min} \quad (13)$$

$$\Delta f = \frac{B}{N_s} \quad (14)$$

In this paper, length of RS sequence is 8. Here, bandwidth  $B$  is divided in somewhat smaller frequency bands, denoted as  $f_1, f_2 \dots$ . Center frequency of each frequency band is denoted as  $f_{c1}, f_{c2} \dots$ . Defining  $n_i$  as hopping sequence of user  $i$ ,  $f_{user_i}$  which is applied frequency of user  $i$  is represented by

$$f_{user_{i_k}} = (f_{n_{i_k}(1)}, f_{n_{i_k}(2)}, \dots, f_{n_{i_k}(j)} \dots) \quad (15)$$

Chirping rate is represented by

$$\mu = \frac{\Delta f}{T} \quad (16)$$

$$T = 2\tau \quad (17)$$

Here,  $\tau$  denotes pulse width. Finally, chirp pulse waveform of the  $j$ -th chip for the  $i$ -th user,  $s_{i_k,j}(t)$ , is represented as

$$s_{i_k,j}(t) = \begin{cases} r(t - \frac{T}{2}) \exp(-j\omega_{i_k,j}(t)) & (0 \leq t \leq T) \\ 0 & (\text{otherwise}) \end{cases} \quad (18)$$

$$\omega_{i_k,j}(t) = 2\pi f_{user_{i_k}(j)}(t - \frac{T}{2}) + (\frac{\pi\mu}{2})(t - \frac{T}{2})^2 \quad (19)$$

Fig.1 illustrates described principle.

Description of the Pulsed chirp UWB receiver is the same as DS-UWB one. This time,  $f_{c1} f_{cNs}$  are defined in table.2, for RS frequency hopping sequences.

**Table 2** Frequency divided each Center Frequency (length of RS sequence 8)

	Center Frequency $f_c$ [GHz]		Center Frequency $f_c$ [GHz]
1	3.2125	5	4.1125
2	3.4375	6	4.3375
3	3.6625	7	4.5625
4	3.8875	8	4.7875

Here, like Fig.1, hopping sequence which is used for parallel transmit defined below.

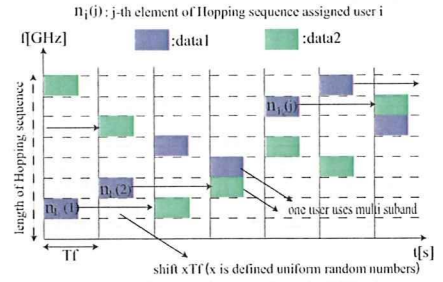


**Fig. 1** Frequency hopping of proposed method .

#### 4. Wearable WBAN

Wearable WBAN is different from usual indoor and outdoor UWB propagation models. Propagation through the body is negligible in the gigahertz frequency range and can be ignored. In the Wearable WBAN, path loss is defined for the  $T_x - R_x$  distance traveled by the wave around the perimeter of the body, not a shortest path distance between transmitter and receiver. Furthermore, in IEEE 802.15.6BAN CM3, this channel model discussed generally characterize the path loss of BAN devices taking into account possible shadowing due to the human body or obstacles near the human body and postures of human body. This channel model's definitions is body surface node is placed on the surface of the human skin or at most 2 centimeters away.

Path loss formula is

$$PL(d)[dB] = a \log_{10}(d) + b + N \quad (20)$$

$a$  and  $b$  are coefficients of linear fitting,  $d$  is  $T_x - R_x$  distance in mm, and  $N$  is normally distributed variable with zero mean and standard deviation  $\sigma_N$ .

In this paper, we consider that effect of interference wave which is asynchronous transmitted (multi pico-net interference). We assume IEEE 802.15.6BAN channel model CM3 with AWGN.

#### 5. Simulation

##### 5.1 Simulation parameter

Simulation setup is shown in table 4 and table 5. Transmitted pulse waveform is root raised cosine pulse with roll-off factor equal to 0.6. In this simulation, we consider multi pico-net interference. At the receiver, the spreading sequence is assumed to be known and it is perfectly synchronized. In this paper, SIR is given by

$$SIR = \frac{\text{the power of wanted wave}}{\text{the power of one interference wave}} \quad (21)$$

**Table 3** Simulation setup of conventional method.

Transmit signal	DS-UWB Chirp on UWB (CoU)
Spread sequence	DS-UWB:gold sequence(length:7)
Frequency band	3-5GHz( $\tau=0.75\text{ns}$ )(DS-UWB) ( $\tau = 3\text{ns}$ )(CoU)
Sampling time	0.08[ns]
Bit rate	1Mbps,3Mbps
Channel model	IEEE15.6BAN CM3

**Table 4** Simulation setup of proposed method

Transmit signal	Pulsed chirp UWB
Spread sequence	Gold sequence(length:7)
Hopping sequence	RS sequence(length:8)
Parallel transmit data	3
Pulse width	2.5[ns]
Frequency band	3-5GHz
Sampling time	0.08[ns]
Bit rate	1Mbps,3Mbps
Channel model	IEEE15.6BAN CM3

## 5.2 Simulation results

The BER (Bit Error Rate) characteristics under multi pico-net interference are shown in Fig.2, Fig.3, Fig.4, Fig.5. Fig.2 and Fig.3 shows BER characteristics in the case of 8 pico-net and comparison conventional with proposed method for medical and non-medical (bit rate is 3Mbps). When SIR is low, Chirp on UWB is superior to others. This is because Chirp on UWB is resistant to near-far problem. When SIR is high, both proposed method which are single hop and parallel hop is superior to conventional methods. Proposed method is combined characteristic of Chirp on UWB and DS-UWB. However, there aren't different single hop's characteristics from parallel hop's characteristics. Since, in the Fig.3, we compare single hop with parallel hop. Fig.3 shows BER characteristics in the case of interference pico-net's number is 3 or 6. When number of interference pico-net is 3, parallel hop is superior to single hop. This is because, when the number of interference pico-net is small, majority rule is more effective. This consideration show Fig.4. In Fig.4, we compare parallel hop with change of interference pico-net number. Fig.4 shows BER characteristics in the case of interference pico-net number is 1,3,6,8. When number of interference pico-net is low, BER characteristics is good performance. Since, in the parallel hop, lower number of interference pico-net, we obtain better performance. Since, these results show that proposed method (parallel hop) is able to consist medical system and non-medical system by using parallel hop. And, proposed method's bit rate which is parallel hop for non-medical use is 3Mbps. However, proposed method's time frame  $T_f$  is shorter than conventional method because of parallel transmit, so proposed method which is parallel hop for non-medical use is concerned with low

duty cycle.

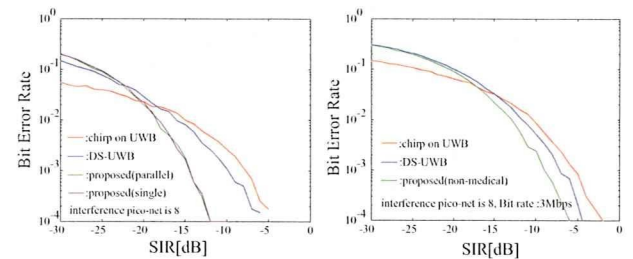


**Fig. 2** Comparison proposed method (medical) with conventional method (non-medical)

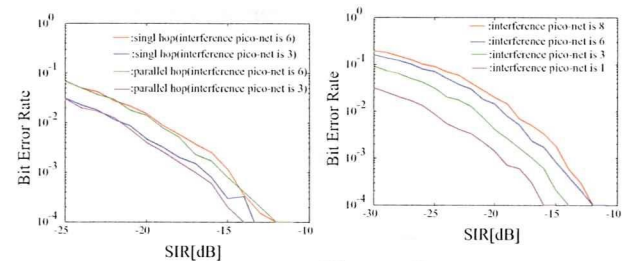


**Fig. 5** Comparison parallel hop with parallel hop (medical)

## 6. Conclusions

In this paper, we are compared proposed method of Pulsed chirp UWB with single hop or parallel hop with conventional methods of UWB IR. Both proposed methods single hop and parallel hop are superior to conventional methods. Especially in the case of interference pico-net numbers is low, proposed method which is parallel hop is superior to conventional method and proposed method which is single hop. Furthermore, proposed method which is parallel hop is able to consist medical system and non-medical system. For a future research, we will consider interference to and from narrowband system and we will consider effect of low duty cycle which is parallel hop for non-medical use.

## reference

- [1] Andrew Fort, Julien Ryckaert, Claude Desset, Philippe De Doncker, Piet Wambacq, Leo Van Biesen, "Ultra-Wideband Channel Model for Communication Around the Human Body" 0733-8716, 2006 IEEE
- [2] Huaping Liu, "Multicode Ultra-Wideband Scheme Using Chirp Waveforms", IEEE JOURNAL ON SELECTED AREAS IN COMMUNICATIONS, VOL.24,NO.4,APRIL2006
- [3] IEEE P802.15 Working Group for Wireless Personal Area Networks(WPANs), NICT Phy Solution:Part 1: Chirp Pulse Based IR-UWB Physical Layer, IEEE 15-09-0166-01-0006, 10 March 2009

# Hybrid ARQ Error-Controlling Scheme for Robust and Efficient Transmission of a UWB Body Area Network

Haruka Suzuki

The Division of Physics, Electrical and  
Computer Engineering,  
Yokohama National University (YNU),  
Yokohama-city, JAPAN.

Marco Hernandez

Medical ICT Group, National Institute of  
Information and Communications  
Technology (NICT),  
Yokohama-city, JAPAN.

Ryuji Kohno

Yokohama National University (YNU),  
National Institute of Information and  
Communications Technology (NICT),  
Yokohama-city, JAPAN.

**Abstract**— This paper presents hybrid type-II automatic repeat request (H-ARQ) for wireless wearable body area networks (BANs) based on ultra wideband (UWB) technology. The proposed model is based on three schemes, namely, high rate optimized rate compatible punctured convolutional codes (HRO-RCPC), Reed Solomon (RS) invertible codes and their concatenation. The performance is investigated for different channels: CM3 and CM4 scenarios of IEEE802.15.6 for standard of BAN. It is shown that the improvement in performance in terms of throughput and error protection robustness is very significant. Thus, the proposed H-ARQ schemes can be employed and optimized to suit medical and non-medical applications.

## I. INTRODUCTION

Body area networks (BANs) have emerged as an important subject in personal wireless communications, recently. Indeed, the standardization task group IEEE 802.15.6 pursues the standardization of PHY and MAC layers for BANs nowadays. The potential mass market includes medical and non-medical applications. As they require different quality of service (QoS) in terms of reliability and performance, a fixed error control mechanism like forward error correction (FEC) is not appropriate. Most cases of non-medical applications do not require strong error control but less complexity and power consumption, and in the special case of video transmission a large throughput and low latency are needed. On the contrary, medical applications require high reliability and relative low data rate transmission as well high data rate transmission. Hence, strong error control is expected while relatively larger complexity is allowed. Thus, in order to reconcile between medical and non-medical applications requirements, we propose an adaptive error control mechanism in the form of hybrid type II ARQ (H-ARQ). Such error system adapts to the channel conditions which can optimize the throughput, latency and reliability according to the application specification and channel conditions.

Practical implementations of UWB systems for BANs with current technology are non-coherent architectures.

Indeed, BAN devices require very low power consumption due to constraint imposed by battery's power and lifespan. In contrast, coherent transceivers in the UWB regime demand high power consumption. Therefore, we propose a simple and practical 2PPM modulation scheme with energy detection at the receiver. This makes it feasible to implement an analog front-end at the receiver (with low power consumption) in the high band of UWB, where UWB-BANs are proposed to operate, globally. In this paper, it is assumed that interference among coexisting piconets BANs, because a coordinator in each piconet BAN of IEEE802.15.6 can control access of all the devices within its coordinating piconet so as to avoid contention among accesses of all the devices although interference among coexisting piconet BANs due to asynchronous access among the coexisting piconets. Since high band of UWB regulation such as 7.25-10.25GHz has suppressed interference enough low to coexisting other radios. However, non-coherent transceivers have poorer performance than coherent architectures. Therefore, it is necessary to introduce an error control mechanism that can guarantee QoS and performance depending on the application and channel condition, while relying in a simple UWB-PHY.

We study three forms of HARQ for BANs, namely, hybrid type II ARQ based on half-rate invertible coding and concatenated coding. The rest of the paper is divided as follows: Section II delineates the system and the signal. Section III illustrates hybrid type II ARQ proposal, which is based on RCPC and invertible codes, Section IV shows simulation results and evaluates their performances. Such simulation results are presented for the scenarios CM3 (on-body to on-body devices) and CM4 (on-body to a gateway)[1]. Finally, Section V conclusions are drawn.

## II. SYSTEM MODEL OF WIRELESS BODY AREA NETWORK

### A. System Model

Medical and non-medical applications need to coexist in BANs. As the network topology is star, the communication links are performed between on-body or in-body devices and

a single central controller or coordinator. In particular, the communication link for medical applications require higher reliability or QoS in contrast to non-medical applications as shown Table I. Consequently, it increasing QoS means to increase complexity and power consumption.

TABLE I. QoS REQUIREMENT

Devices	Data storage	Real-time
Main usage	Storage medical data	Healthcare, Games, Emergency call
Bit error rate	$\leq 10^{-6}$	$\leq 10^{-3}$
Data rate	100kbps-10Mbps	1-10Mbps
Key requirement	Reliability	Latency

As HARQ combines FEC and retransmission, the main purpose is to design the FEC such that it corrects the error patterns that appear frequently in the channel. The FEC is maintained with low complexity as much as possible. On the other hand, when error patterns that appear less frequently like time-varying behavior and/or deep fades, a retransmission is requested. Hence, a fine balance between throughput and error correction is achieved, which makes the system is more reliable. This is only required for high QoS medical applications. Hence, in order to harmonize medical a non-medical applications, we propose that non-medical devices employ only FEC and medical devices are HARQ enable, i.e., incremental redundancy and retransmissions are allowed. The maximum number of retransmissions is bounded to end-to-end delay or latency of the system. Currently, such latency parameter is under study in the IEEE 802.15.6 TG.

### B. Signal Model

The transmitting UWB signal is given by

$$x(t) = \sum_m w(t - g_m T_{BPM} - mT_{sym}) \quad (1)$$

$$w(t) = \sum_{n=0}^{N_{cpb}-1} d_{m,n} p(t - nT_c) \quad (2)$$

where  $g_m \in \{0,1\}$  is the  $m$ th component of a given codeword,  $T_{BPM}$  is the slot time for 2PPM or burst position modulation,  $T_{sym}$  is the 2PPM symbol time. The basis function  $w(t)$  is a burst of pulses  $p(t)$ , where  $d_{m,n}$  is a scrambling sequence. This is only to control data rate and legacy to IEEE 802.15.4a systems.

## III. TYPE II HYBRID ARQ SCHEME FOR WBAN

### A. Proposed System configuration

As mentioned above, the proposed system is HARQ type II. In such scheme, only parity bits are sent some retransmissions. Erroneous packets are not discarded and the decoder can employ previously received packets. The main characteristics are requires low coding overhead and is suitable for bursty (time-varying) channels. Figures 1 shows the system model of the proposed system. In our proposed system, both of the medical and non-medical applications use the same modulation and demodulation schemes. But only the medical application has a H-ARQ function. Hence, when

the lack of the reliability has detected, the medical devices can request a retransmission.

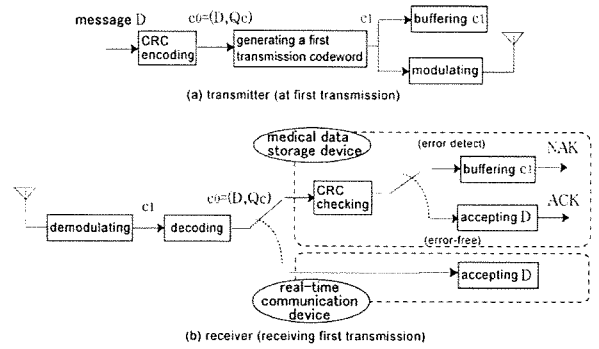


Figure 1. Proposed system model

### B. Proposed system using Concatenated Coding

The idea is to start with RS-based HARQ for the first transmission (information bits) and first retransmission (parity bits). So the non-medical devices is not needed to have the function of decoding. It is different from the generic H-ARQ in satellite communications and so on. In order to improve performance, we propose to use concatenated coding with RS\$(n,k)\$ as outer codes and RCPC as inner codes. If the algorithm determines that the error pattern cannot be corrected, then information bits and RS parity bits are concatenated with RCPC coding. Consequently, if errors cannot be corrected in this fashion, incremental redundancy is applied. Figure 2 shows the flow of the proposed scheme.

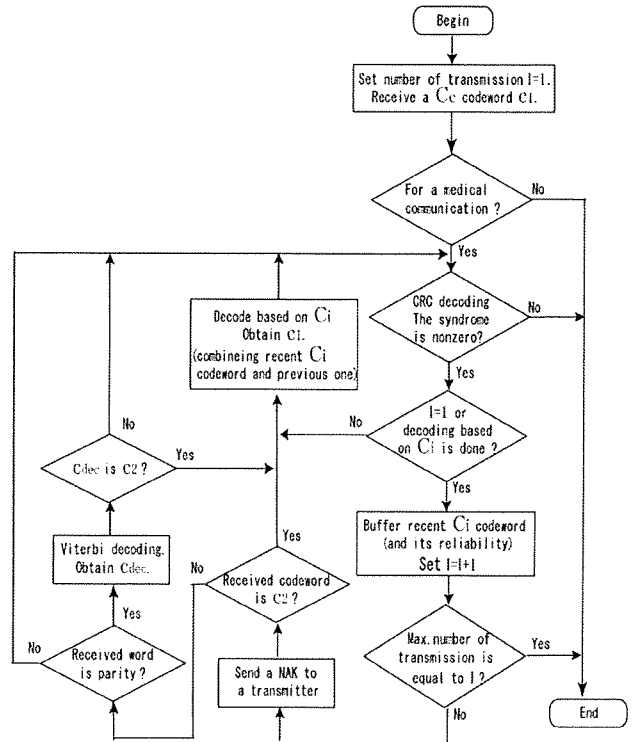


Figure 2. Flow chart of the proposed system

First, a message  $D$  is encoded with  $C_c$  that written by  $c_0 = (D, Q_c)$ , where  $Q_c$  is CRC parity bits and codeword  $c_1 = (c_0)$  is the first transmission codeword the we obtain. If any other FEC is needed,  $c_1$  become  $c_1 = (c_0, Q)$  where  $Q$  denotes the any other FEC parity-bits. Let  $\hat{c}_1 = (\hat{c}_0)$  denotes a received first codeword. While the non-medical application receiver is finishing the communication, but the medical application receiver computes the syndrome of  $\hat{c}_0 = (\hat{D}, \hat{Q}_c)$  based on  $C_c$ .

After receiving this NAK, the transmitter encodes the first transmission codeword  $c_1$  with  $C_i$ , a codeword  $(c_1, Q_i)$ . with  $C_i$ . Then a retransmission codeword  $c_2 = (Q_i)$ , where  $Q_i$  denotes invertible (RS) parity bits, is obtained. After that, the same operation as mentioned above is redone. Since the syndrome is nonzero, also the erroneous codeword  $\hat{c}_2$  is saved in the receiver. Once a NAK is sent back to the transmitter, the next retransmission word is RCPC parity bits. The transmitter then encodes the  $c_1$  with systematic RCPC codes obtaining a codeword  $(c_1, Q_{p1})$ , where  $Q_{p1}$  denotes RCPC parity bits based on the  $c_1$ . Thus, a retransmission word  $c_{p1} = (Q_{p1})$  is generated. After receiving  $\hat{c}_{p1}$ ,  $\hat{c}_{p1}$  is combined with  $\hat{c}_1$  obtaining a codeword  $(\hat{c}_1, \hat{Q}_{p1})$ . We can get more reliable codeword  $\hat{c}_1'$  by viterbi decoding. The  $\hat{c}_1'$  is saved in the receiver and a NAK is sent to the transmitter even if the syndrome is nonzero. In addition, the transmitter also encodes the  $c_2$  with systematic RCPC codes obtaining a codeword  $(c_2, Q_{p2})$ , where  $Q_{p2}$  denotes RCPC parity bits based on the  $c_2$ . The same process as mentioned above is again redone. A transmitter repeats retransmission  $c_1, c_2, c_{p1}, c_{p2}$  until the message  $D$  is error-free and consequently accepted. We can see later from the results that when a receiver has a function of decoding with a reliability of decoded codeword based on  $C_i$ , the system throughput can achieve more improvement. It is our future work.

#### IV. PERFORMANCE EVALUATION

Figures 3-8 show the performances of our proposed system using RS-based and concatenated-based H-ARQ. Simulation parameters are given in Table 2.

TABLE II. SIMULATION PARAMETERS

Channel	IEEE802.15.6 CM3 and CM4
Mod.Demod.	2PPM, Energy detection
Pulse shape, duration	Modulated RRC, 2nsec
Bit rate	2Mbps
CRC codes	CRC-CCITT (parity bits length=16bits)
FEC	$C_i : GF(2^4), (15, 7)RS$ codes, code rate=0.467. $C_i : GF(2^5), (31, 15)RS$ codes, code rate=0.484. Parent code rate 1/2, constraint length 3, Systematic RCPC codes
Decoding	Bounded distance decoding Hard decision Viterbi decoding
Block length	300 bits (containing CRC codeword)
Max.Number of retransmission	RS-based:1, concatenated-based:1,2,3

We assume the throughput efficiency is computed by

$$\eta = (1 - \text{PER}) * K/N \quad (3)$$

where PER denotes packet error rate,  $K$  and  $N$  denote transmitted message bits length and total transmitted message bits length, respectively. Hence, the throughput efficiency shows the average of error-free data communications. And we define the data rate as the number of data bits per second. With coding, the parity bits are also transmitted, so the data rate is not equal to the bit rate. For the non-medical communication, the data rate is the same as the bit rate, because the first transmitting codeword contains only the parity bits of CRC codes.  $I$  and  $I_{\max}$  denote the number of transmission and the max number of transmission, respectively.

For comparing, the results of convolutional codes with code rate of 1/3 and the constraint length of 3 are shown. Simulation Results

#### A. Performance Evaluation

Figures 3 and 6 show the good performance of the concatenated-based H-ARQ ( $I=4$ ) as its achieved the bit error rate  $\text{BER} = 10^{-6}$  at  $\text{SNR} = 13.5$  dB due to its viterbi decoding and code rate. The non coded one is the first

##### 1) CM3 (on-body to on-body devices)

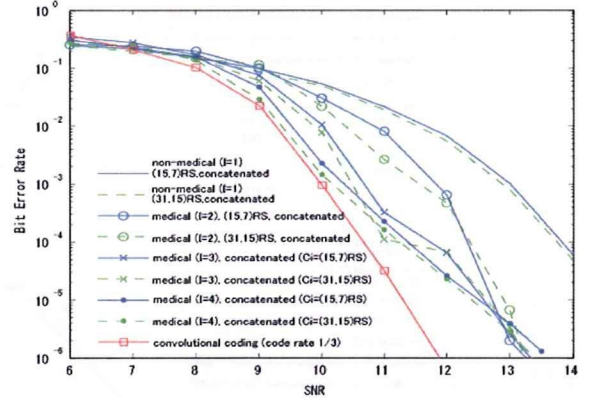


Figure 3. Bit error rate for medical and non-medical applications in the CM3 channel.

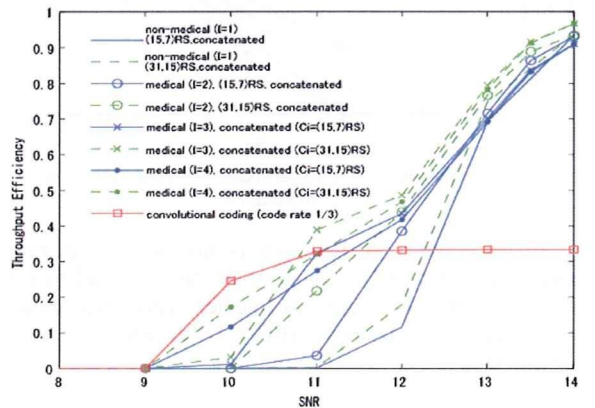


Figure 4. Throughput for medical and non-medical applications in the CM3 channel.



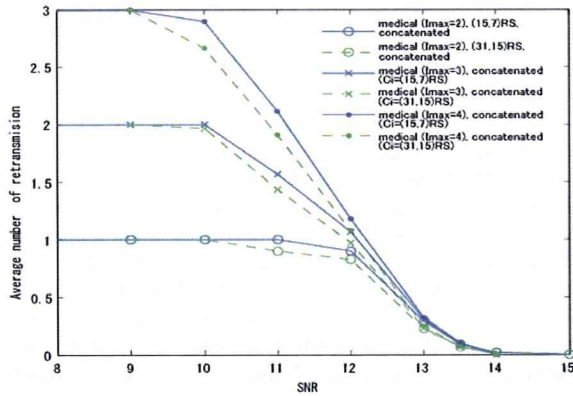


Figure 5. Average number of retransmission for medical applications in the CM3 channel.

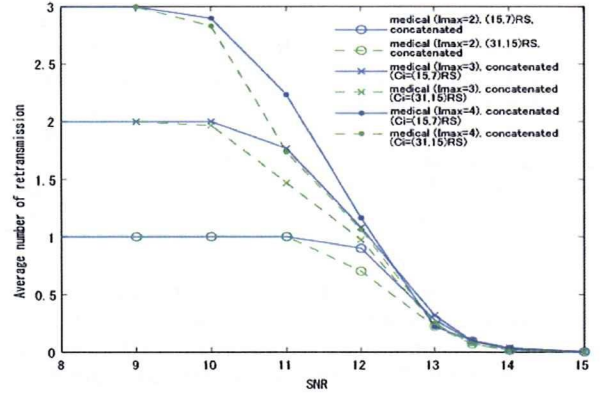


Figure 8. Average number of retransmission for medical applications in the CM3 channel.

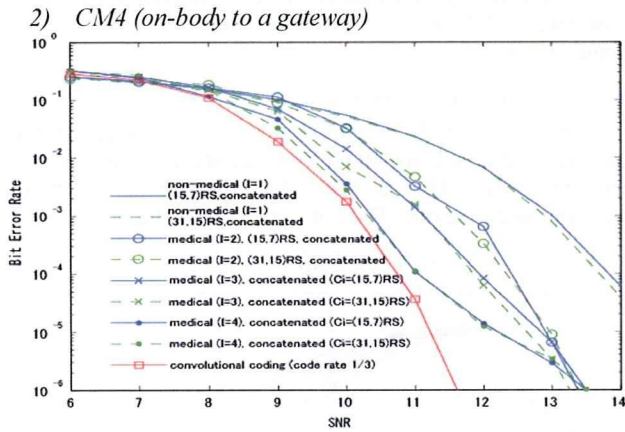


Figure 6. Bit error rate for medical and non-medical applications in the CM3 channel.

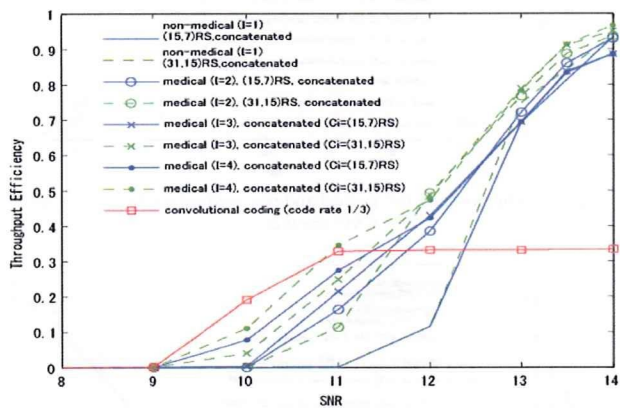


Figure 7. Throughput for medical and non-medical applications in the CM3 channel.

transmission of the RS-based is same as the concatenated-based one. The BER of non coded one is equal to  $10^{-3}$  at SNR = 13 dB. Therefore, the medical communications can satisfy its QoS by using H-ARQ function while the bit rate is not changed.

From figures 4-5, 7-8 at the low SNR, because of the PER of the concatenated-based ( $I=4$ ) is very low, the throughput efficiency of the concatenated-based ( $I=4$ ) is better than the RS-based ( $I=2$ ). At the first retransmission, the information and CRC parity bits length of every codeword are the same. Then, at the high SNR, all cases achieve the same throughput efficiency. And the average number of retransmission also converges. Hence, the proposed scheme adapts to the channel. The performance when only using convolutional codes with code rate  $1/3$  also achieves the good BER performance. But if the bit rate remains 2Mbps, the data rate becomes  $2/3$ Mbps. Furthermore, the throughput efficiency is still  $1/3$  at the high SNR. To summarize, the proposed concatenated scheme is more suitable for the low complexity of the non-medical receivers and the high reliability of the medical communications.

## V. CONCLUSIONS

This study researched hybrid type II H-ARQ techniques for BANs. The signaling scheme is IR-UWB in the high band of UWB with 2PPM and energy detection. The investigated H-ARQs are based on invertible codes. Simulations results show that good performance in UWB-BAN channels can be achieved by using concatenated codes which we proposed. Hence, the proposed schemes shows that a robust scheme is possible for medical data storage applications of BANs without ruining efficiency of data rate for real-time applications.

## REFERENCES

- [1] "Body Area Network Channel Model Document," IEEE P802.15-08-0780-0x-0006[Online], Available: <https://mentor.ieee.org/802.15/documents>.
- [2] S. Lin, P. Yu., "A Hybrid ARQ with Parity Retransmission for Error Control of Satellite Channels," IEEE Transactions on Communications, Vol 30, No 7, July 1982, pp. 1701-1719.
- [3] J. Hagenauer, "Rate-Compatible Punctured Convolutional Codes," IEEE Transactions on Communications, Vol 36, No 4, April 1988, pp. 389-400.
- [4] S. Lin, D. J. Costello Jr., ErrorControl Coding: Fundamental and Applications, Prentice-Hall, Englewood Cliffs NJ, 1983.

# 医療・非医療用ボディアエリアネットワークに適した Hybrid ARQ Type2 誤り制御法

TYPE-2 HYBRID ARQ SCHEME FOR ERROR CONTROL OF WIRELESS BODY AREA NETWORK

鈴木晴香<sup>1</sup>  
Haruka SUZUKI

林雅之<sup>1</sup>  
Masayuki HAYASHI

河野隆二<sup>1</sup>  
Ryuji KOHNO

横浜国立大学大学院 工学府<sup>1</sup>  
Graduate School of Engineering, Yokohama National University

## 1 はじめに

医療もしくはヘルスケア・エンタテインメント用途を目的とし人体内部や体表に装着された端末で構成されるネットワーク, WBAN(wireless body area network)が近年注目されている. しかし医療用途の場合は信頼性の高い通信が求められ, ヘルスケア・エンタテインメント用途の場合はリアルタイム通信が要求されるため, 一般には同じ端末での両用途の両立は回路の複雑化を招き WBAN に適さない. そこで本稿では, 変調・符号化法などの送信側は同一のまま, 受信側の誤り制御法を切り替えることで両用途の要求を達成することを考える.

## 2 システムモデル

人体内部や体表で用いられるため, 端末は低消費電力で小型化が求められる. したがって通信方式は UWB-IR(ultra wideband impulse radio) を, 変復調にはパルス位置変調, エネルギー検波を適用する. システムモデルを図 1 に示す.

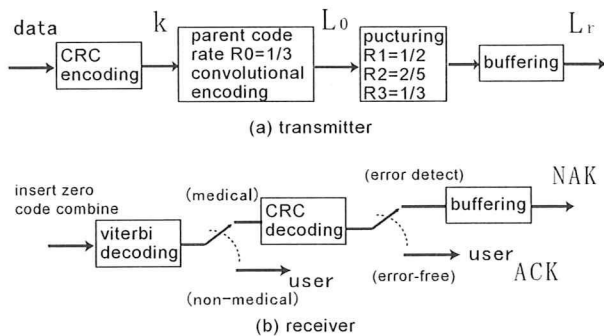


図 1 提案システムモデル

まずデータ  $k$  ビットに誤り検出のため CRC16 ビットを付加し, その後原符号化率  $R_0 = 1/3$  で畳込み符号化を行い符号語  $L_0$  を得る. 次にパンクチャドパターン ([1]) を用い符号語  $L_0$  をパンクチャドし, 符号語  $L_r$  に含まれる冗長ビットを符号語  $L_{r+1}$  は含まないような符号語  $L_1, L_2, L_3$  を得る. 医療用のみ誤りを検出したとき ARQ(automatic repeat-request) 機能を用い再送が要求され,  $r$  回目の送信時は符号化率  $R_r (R_1 = 1/2, R_2 = 2/5, R_3 = 1/3)$  の冗長度となる. このような符号化率が可変な畳込み符号は RCPC(rate-compatible punctured convolutional) 符号とよばれる. 非医療用の場合は符号化率  $R_1 = 1/2$  の畳込み符号の冗長度となる.

## 3 評価

以下の諸元を用いて, 計算機シミュレーションにより提案システムのスループット特性を導出した.

表 1 提案システムモデルのシミュレーション諸元

通信路	WBAN チャンネルモデル (CM3)
情報ビット長	300[bits](終端, CRC ビット含む)
復号法	硬判定ビタビ復号
ARQ	Selective-Repeat ARQ
使用帯域幅	500MHz
シンボルレート	4Mbps

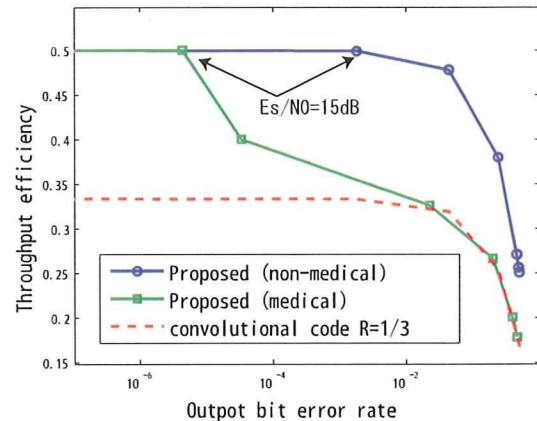


図 2 復号誤り率対スループット効率

$E_s/N_0$  が 15dB 以上でそれぞれの所望誤り率  $10^{-6}, 10^{-3}$  を満たし, さらに伝送速度 2Mbps を達成している. よって本提案が有効であることが示せた.

## 4 むすび

今回はいずれの受信器もビタビ復号機能を有することを想定した. 今後の検討として, 訂正機能をもたないより簡易な受信器も通信可能とするシステムの構築が挙げられる.

## 参考文献

- [1] S.Falahati, T.Ottosson "Convolutional Coding and Decoding in Hybrid Type-II ARQ Schemes on Wireless Channels", IEEE VTC, 1999
- [2] S.Lin, Yu, P. "A Hybrid ARQ Scheme with Parity Retransmission for Error Control of Satellite Channels", IEEE Transactions, 1982

# WBANに適した高信頼度医療用通信方式の研究

Study on High Quality Medical Transmission Schemes for a WBAN

望月英希  
Hideki Mochizuki

河野隆二  
Ryuji Kohno

横浜国立大学大学院工学府物理情報工学専攻  
Division of Electrical and Computer Engineering, Faculty of Engineering, Yokohama National University

## 1 はじめに

近年、情報通信技術を医療分野へ応用する研究が注目されている。その中でも体表に装着された端末によってのみ構成されるネットワークである、ウェアラブルWBAN(Wireless Body Area Network)に注目する。その中でも特に、医療用として用いる場合、生体情報を扱うため高信頼度な通信方式が必要と考えられる。本稿では高信頼度な通信を実現するために、使用周波数をサブバンド化し、ホッピング系列を用いて送信波形を作成する。そしてその送信波を同じ data で並列送信することで高信頼度な通信を実現する方式を提案する。また、干渉波として他ピコネットからの非同期干渉による影響を考え、計算機シミュレーションにより既存法(DS-UWB, Chirp-on-UWB)と提案法の比較評価を行う。

## 2 提案方式

本稿では、使用周波数帯域を用いるホッピング系列の周期で分割し、ホッピング系列によって、使用周波数帯を決定してパルスを Chirp させる。そして、そのそれぞれの Chirp パルス波形を直接拡散し並列送信する方式を提案する。以下詳細を示す。

送信する送信波形を  $f(t)$  とすると、 $f(t)$  は次のように表される。

$$f(t) = \sum_{k=1}^{d_s} \sum_{j=0}^{N_s-1} m_{i,j} (s_{i_k,j}(t - jT_f)) \quad (1)$$
$$(c_{i,j} = 1 \text{ のとき } m_{i,j} = 1, c_{i,j} = 0 \text{ のとき } m_{i,j} = -1)$$

この時、 $c_{i,j}$  はユーザ  $i$  に割り当てられた PN 系列であり、 $N_s$  は PN 系列の系列長である。また、 $d_s$  は並列送信数で、 $s_{i,j}$  はユーザ  $i$  の  $j$  番目の Chirp パルス波形である。この Chirp パルス波形  $s_{i,j}$  は次のように表す。

$$s_{i_k,j}(t) = \begin{cases} r(t - \frac{T}{2}) \exp(-j\omega_{i_k,j}(t)) & (0 \leq t \leq T) \\ 0 & (\text{otherwise}) \end{cases} \quad (2)$$

$$\omega_{i_k,j}(t) = 2\pi f_{user_{i_k}(j)}(t - \frac{T}{2}) + (\frac{\pi\mu}{2})(t - \frac{T}{2})^2 \quad (3)$$

ここで  $f_{user_{i_k}}$  は式 (4) のように表され、 $\mu_{i,j}$  はユーザ  $i$  の  $j$  番目の波形の周波数挿引率であり、式 (5) のように表される。

$$f_{user_{i_k}} = (f_{n_{i_k}(1)}, f_{n_{i_k}(2)}, \dots, f_{n_{i_k}(j)} \dots) \quad (4)$$

$n_{i_k}$  はユーザ  $i$  の  $k$  番目の並列送信に利用するホッピング系列である。また、周波数挿引率は次のように表すことができる。

$$\mu = \frac{\Delta f}{T} \quad (5)$$

$$T = 2\tau \quad (6)$$

## 3 性能評価

本稿で想定しているウェアラブル WBAN 環境下では、所望波が激しく減衰してしまう [1]。そのため、今回は IEEE15.6BAN のチャンネルモデルを使用して性能評価を行った。SIR が非常に  $-30 \sim -20$  dB 程度の非常に低い範囲では、遠近問題に耐性のある Chirp-on-UWB 方式の特性が良いが、SIR がそれよりも高い範囲では提案方式の特性が既存方式と比較して優れており、高信頼度な通信が可能であることが確認できた。

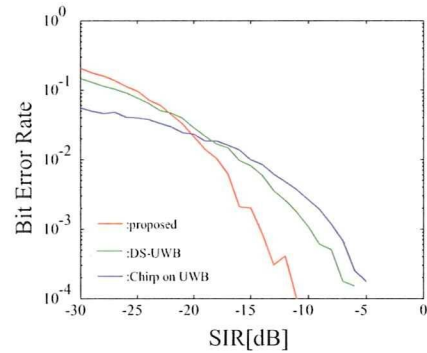


図1 干渉ピコネット数が8の時の比較 (通信速度 1Mbps)

## 4 まとめ

高信頼度医療用通信を実現するために方式を提案し、特性を確認した。今後は、MAC プロトコルを考慮した検討が必要である。

## 参考文献

- [1] Andrew Fort, Julien Ryckaert, Claude Dessel, Philippe De Doncker, Piet Wambacq, Leo Van Biesen, "Ultra-Wideband Channel Model for Communication Around the Human Body" 0733-8716, 2006 IEEE

# 時間反転波による電磁波ハイパーサーミアの減衰補償法の検討

Attenuation Compensation Method for Electromagnetic Wave Hyperthermia using Time Reversal Wave

三浦 英朗  
Hideaki Miura

河野 隆二  
Ryuji Kohno

横浜国立大学大学院工学府物理情報工学専攻  
Division of Electrical and Computer Engineering, Faculty of Engineering, Yokohama National University

## 1 はじめに

近年、がんの治療方法に関してハイパーサーミアという温熱療法が注目されている。ハイパーサーミアとはがん組織が正常細胞に比べて熱に弱いということを利用してがんを死滅させるという治療法である。

そこで、この治療法で熱を加える手法として、体外から電磁波を時間反転波として照射する方法を用いる。しかし、生体内では電磁波は減衰が生じてしまい、その影響によって焦点が形成されないという現象が生じる。本稿では体内での減衰の影響を考慮し、補償法を適用することによって適切な温度分布を得ることができることを示す。

## 2 時間反転波ハイパーサーミアについて

時間反転波とはもともと光学の分野で使われてきた技術であり [1]、これをハイパーサーミアに応用することを考える。乳がんを想定したモデルを用いて、がんの位置は MRI などの診断により既知であるとする。

時間反転波をハイパーサーミアに用いる手順としては、まず乳房の周囲に 16 素子を配置した場合を想定し、その 1 素子から非常に短いパルス波の Pilot 信号を送信する。この信号は体内を伝搬してがんにおいて反射、散乱を起こし、この反射波を体外の 16 点の素子で受信する。これを時間反転処理して全素子から体内に再送信することにより、がんの位置で焦点が形成することができる。これは時間反転波の性質である、最も強く散乱された点に波が集中することを応用している。

## 3 短時間フーリエ変換による減衰補償について

減衰は一般にフィルタのように働き、その影響を除去するには逆特性のフィルタを用いればよいと言われている。そこで本稿では生体を対象とするために組織の誘電率などは既知ではないという状況での評価を行う。つまり減衰の大きさを求める必要がある。そこで、減衰については周波数依存性があるので次のように求める。

$$S(d, \omega) = \frac{1}{\sqrt{d}} e^{-(\alpha(\omega) + j\beta(\omega))d} \quad (1)$$

ここで  $d$  は伝搬距離、 $\alpha$  は減衰定数、 $\beta$  は位相定数を表し、大まかに減衰量を推定する。減衰補償では周波数帯と到達時間の違いによって減衰量が異なる。そのため簡易な時間依存のフィルタリングとして短時間フーリエ変換を用い、減衰量の補償を行う。そのブロック図を以下に示す。

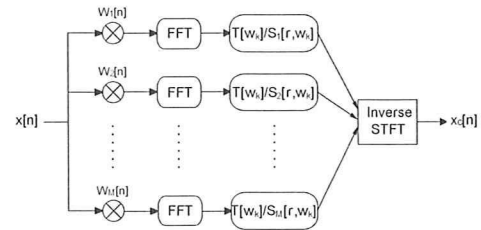


図 1 減衰補償のブロック図

以上のように周波数領域において減衰量の逆特性をかけ、さらに高周波数帯の強調を防ぐために、送信パイロット信号もかけ合わせることをとする。以上のような補償を用いて、電界分布を FDTD 法により計算して生体熱輸送方程式を用いてモデルの温度分布を算出する。その温度分布の結果を以下に示す。

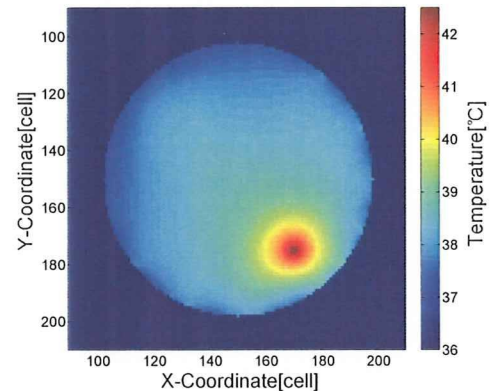


図 2 温度分布の結果

## 4 考察とまとめ

結果のグラフから、時間反転波による手法によってがんの全領域においてハイパーサーミアに必要とされる  $42.5^\circ\text{C}$  以上の温度に到達しているということがわかる。これは時間反転波の理論が理想的な点散乱を仮定しているものであり、がんの大きさによってはうまく焦点が集中しないということも考えられる。今後の検討として、がんの大きさを変えたことによる影響、またより現実に近いモデルを用いた際の影響についても考えていく必要があると思われる。

## 参考文献

- [1] G. Lerosey, J. de Rosny, A. Tourin, A. Derode, G. Montaldo, and M. Fink, "Time reversal of electromagnetic waves," *Physical Review Letters*, vol. 92, May 2004.